Projected Unrestricted Hartree−Fock Calculations and the Magnetism of Large Nickel Clusters

Guillermina Lucia Estiú

CEQUINOR, Departamento de Quimica, Facultad de Ciencias Exactas, Universidad Nacional de La Plata, CC 962, CP 1900, La Plata, Argentina

Marshall G. Cory and Michael C. Zerner*

Quantum Theory Project, University of Florida, Gainesville, Florida 32611

Received: June 8, 1999; In Final Form: October 21, 1999

The study of the multiplicity (*M*) of transition metal clusters of different sizes has been motivated by its importance in relation to the reactivity of the structures. For this reason, the accuracy and utility of restricted and unrestricted HF methodologies have been extensively analyzed. We compare rather time-consuming restricted open-shell Hartree−Fock calculations followed by multireference CI (ROHF/MRCI) with fully projected unrestricted Hartree−Fock (PUHF) methodologies for the evaluation of the *M* of small Ni_n clusters ($n = 4, 6, 8, 13$) using the intermediate neglect of differential overlap model Hamiltonian (INDO). Different geometry and lattice parameters are considered, searching for the best way of dealing with the open-shell electronic distributions that are strongly related to reactivity. We examine both the optimized, most stable structures, and those associated with the observed interatomic bulk distance. Our results are compared with those obtained from density functional and ab initio calculations, as well as with experimental data, when available. On the basis of the results of this comparison, the PUHF model is applied to the study of trilayer and bilayer surface-slab Ni clusters of 20 and 51 atoms, respectively.

1. Introduction

Research on the properties of transition metal (TM) clusters has increased in importance, due to application in several fields of chemistry,[1−6] physics,[7−10] and other closely related sciences.[11] Although studies have been most frequently motivated by the resolution of heterogeneous catalysis and/or electronic problems, it has also became significant in biology where TM atoms, very often linked by oxygen or sulfur bridges, define the active sites for enzymatic reaction in metalloproteins.[12−14]

Whereas organometallic structures or metallic oxides are usually present in electronic materials, semi-infinite slabs of transition metals or metallic oxides, as well as nanometric TM structures, play their role in heterogeneous catalysis. Moreover, the possibility of assembling clusters for the design of new materials is also appearing as a promising area.[15]

The detailed experimental knowledge of the relevant characteristics of TM clusters has been largely favored by the development of new spectroscopic techniques. Whereas the symmetry and geometry of small to medium size clusters are indirectly determined by chemical saturation with noninvasive gases, followed by mass spectroscopy,[16] high-resolution spectroscopic techniques are being applied to the characterization of TM dimers and trimers.[17,18]

Within this general scheme, the elucidation of the electronic structure of the different forms associated with the occurrence of TM clusters in nature (surfaces, nanometric particles, or organometallics) becomes a relevant step in understanding the chemistry of the processes in which they are involved. However, the application of quantum chemical procedures to this objective has been marked by both methodological and computational limitations, mainly related to the treatment of a large number of spin states, very close in energy, that sometimes precludes the definite assignment of the state of lowest energy. This statement is particularly true when dealing with nanometric clusters, where the geometry and multiplicity of the structure calculated as most stable, for a given cluster size, still remains dependent on the calculation procedure.[7,19−22] Even within a given methodology, different basis sets in an ab initio or density functional calculation result in different geometries for a given cluster size, and the associated electronic descriptions will not be, thence, even comparable.

Understanding the equilibrium geometry and electronic structure of clusters is not a simple matter. The possible coexistence of two or more isomers (with different properties) for some cluster sizes,[23,24] and the existence of multiple minima on the potential energy surface, the complexity of which increases as the cluster size increases, has restricted the use of first principle studies to clusters containing only a few atoms.[7,20,21,25,26] The problem is even harder in TM clusters, as the highest occupied molecular orbitals are characterized by large degeneracies. This complexity arises from the behavior of the valence electrons, which are occupying short range open d-shells, and highly delocalized 4s orbitals, close in energy to them.

The choice of the theoretical procedure for their treatment is mostly determined by the size of the cluster that is necessary to model the system and the information that should be derived. Whereas molecular dynamic calculations[15,27] can be applied for the elucidation of the geometry, the study of the electronic properties, such as the multiplicity (*M*), needs a consideration of as much electronic correlation as possible. Besides, the study of the *M* of TM clusters becomes relevant for its relation with the activity.

10.1021/jp991863l CCC: $19.00
Published on Web 12/10/1999

Restricted Hartree−Fock methodologies are not considered a good starting point for the treatment of TM clusters. They require a great deal of electron correlation, a consequence of the weak coupling between d orbitals. Ab initio calculations should be, thence, of the very highest quality, and become, for this reason, prohibitive, or, at least, limited to very small systems. Semiempirical self-consistent field (SCF) methods followed by multireference configuration interaction (CI) procedures restricted to single excitations (MR-CIS) have been found to be successful for the treatment of small clusters,[19] but the best way of dealing with more than ten TM atoms is still a matter of investigation. The size of the CI large enough to properly model the multiplicity of these clusters is still an open question. Preliminary studies suggest that the size of the necessary CI is prohibitive.

Density functional (DFT) techniques, including exchange correlation through local and, more accurately, nonlocal (gradient corrected) functionals, seem to successfully deal with both the geometry and the electronic characteristics of small size TM clusters.[21,22,25,26] A high-spin ground state has been found for a 13-atom Ni cluster,[22] but the *M* of larger systems has not been yet evaluated. DFT calculations ignore, however, spin contamination, and the effect that it has on the results is still unclear. In addition, there is no theory of multiplets for Kohn−Sham DFT: rather one assumes that the Sz value is the *S* value. There is ample evidence now that DFT-based methods favor low spin when compared to Hartree−Fock or limited CI and that these latter methods artificially favor high spin due to too great a repulsion between electrons of different spin compared to those of the same spin, but there is not a lot of comparison against experiment when these methods produce different predictions.[28]

An alternative approach is associated with the use of Unrestricted Hartree−Fock (UHF) methodologies, which are simple and easy to refine through the use of Møller−Plesset type perturbation theory. This refinement of the energy, however, will not be accurate in cases where there are near degeneracies, such as in metal clusters, and does little to correct for spin contamination.

Accepting the challenge of dealing with more than a dozen TM atoms at the UHF level, we have chosen to examine the method of fully projected UHF (PUHF) to obtain states of pure spin for Ni_n clusters ($n = 4, 6, 8, 13, 20, 51$), mainly focusing on the multiplicity (*M*) of lower energy associated with each size and symmetry. For the smaller clusters ($n = 4, 6, 8, 13$) we have considered Ni structures built up on the interatomic bulk distance and on the value derived from a full geometry optimization, comparing the results with previous data derived from ROHF-MRCI calculations,[19] searching for the best way of dealing with the open-shell electronic distributions that are strongly related to reactivity. Larger clusters ($n = 20, 51$) have been used to model trilayer and bilayer surface-like systems. Calculations at the PUHF level have been used to evaluate their capability of modeling the electronic characteristics of bulk metals. The results are compared with those obtained from DFT calculations, ab initio calculations and experiment, whenever the information is available for discussion.

2. Methodology

The advantages and disadvantages of restricted and unrestricted HF methodologies for the treatment of open shell problems have been extensively discussed.[29] Whereas the UHF approach of Pople and Nesbet[30] is accepted as the simplest way of treating open-shell systems at the HF level, it usually does not succeed when a large number of molecular orbitals, which define spatially degenerate states, is involved. Geometry optimization of these systems becomes an insurmountable task at this level. This effect is not guaranteed to be avoided by the application of ROHF calculations, as the nonequivalent occupation of degenerate MO, which destroys the symmetry during the SCF cycles, results in spurious Jahn−Teller (JT) distortions. To avoid this effect, we use a configuration-averaged Hartree−Fock (CAHF) method that has been developed within the ROHF theory for the general case of any number of open-shell orbitals containing any number of electrons.[31,32] Calculations are started, in this way, by a CAHF procedure, with an average *M* for the number of electrons considered. The number of orbitals included in the average is diminished in successive cycles until a minimum, compatible with the degeneracy pattern associated with the symmetry under consideration, is attained. This procedure has been used for both the optimization of the geometry and the electronic calculations. In the last case, the orbitals that belong to the CAHF procedure form the reference for the subsequent spin-projection to obtain pure states by means of a Rumer diagram technique.[33] Subsequent CI can also be performed with those orbitals, allowing for a proper check of the ground state, as well as for the refinement of the total wave function and its properties.

ROHF/MRCI and PUHF calculations have been compared for cluster sizes up to Ni_{13}. PUHF calculations have been used for the analysis of Ni_{20} and Ni_{51} surface models.

For both the restricted and unrestricted HF methodologies we have used the Intermediate Neglect of Differential Overlap (INDO) Hamiltonian available within the ZINDO program package.[34] The INDO/S parametrization[35−37] that reproduces UV−vis spectroscopy at the CIS level of theory has been used in the UHF approach. Both the INDO/S and the INDO/1[35,38] parametrizations have been used, on the other hand, in the ROHF calculations. The latter, which is the appropriate choice for geometry optimizations, utilizes two-center-two-electron integrals that are calculated ab initio.

The geometries of the small clusters have been optimized in the framework of ROHF calculations, avoiding symmetry breaking by means of an adequate definition of double and single occupied orbitals by means of a CAHF approach. For these optimized geometries, ROHF and UHF methodologies have been compared in their accuracy to evaluate the *M* of the structures. Dealing with degenerate systems, the wave function for the ROHF calculations is the result of MRCI procedures.

The optimization of the geometry of the Ni_n clusters (up to $n = 13$), as well as the MRCI calculations for the electronic structure and *M* evaluation, have been previously performed and are already published. Details of the procedure, regarding the number of references, the symmetry imposed on the calculations, and the size of the resulting CI have been already discussed in ref 19. The results are repeated here only for comparative purposes.

Ni_{20} and Ni_{51} clusters have been used to define surface slabs that model (111) single-crystal bulk structures. The models (Figures 1 and 2) have been built on the interatomic bulk parameters.[39]

The UHF wave function, a mixture of several pure-spin states of different *M*, with *S* values $\geq$Sz, suffers from spin contamination. To remove the unwanted spin contamination, we have chosen to use the PUHF method to obtain states of pure spin. The model, based on the work of Harriman,[40] has been described in detail in ref 41. On the basis of the results of the comparative analysis performed for the smaller clusters, this methodology is applied to the study of the large surface-like structures, cases

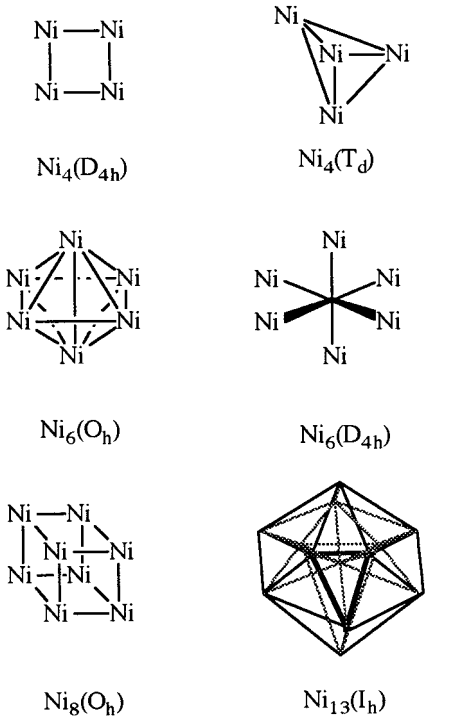

Figure 1. Smaller Ni clusters of this study.

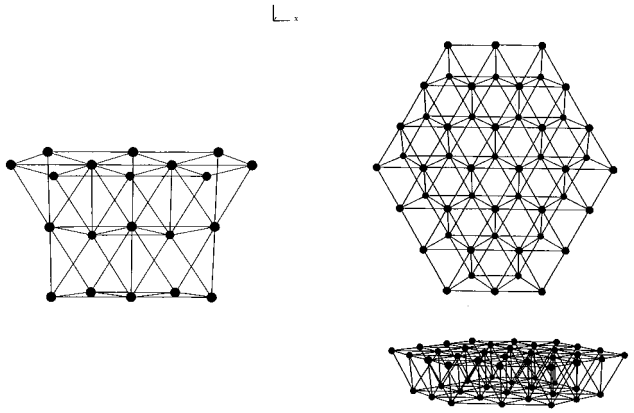

Figure 2. Structures of Ni_{20} and Ni_{51} studied in this work.

in which MRCI is just not feasible. "Weights" are reported in the tables. This is the fraction of each multiplicity in the original UHF wave function. Values close to 1.0 indicate that the UHF function is nearly a pure spin state. More accurate projections are generally expected for states of multiplicity M when that weight in the UHF wave function is close to unity. Smaller weights suggest that the variational optimization of the UHF wave function was less on the multiplicity of interest than those of higher weights. It is rather remarkable that there is a good deal of consistency in the projected energies from UHF wave functions for states of a given M obtained from projections on UHF wave functions of different Sz; see below.

Within the PUHF methodology, different parametrizations of the resonant integrals β have been compared for the surface-like clusters, insofar as they influence the calculated description of these larger clusters.

The two-center one-electron resonance integrals for the valence orbitals is given by

$$\beta^{AB} = (\beta^A + \beta^B)/2 \qquad (2.1)$$

where β^A and β^B are parameters specific for the same type of orbital on each of the atoms involved. The influence of the β^{AB} value on the calculated energy of the molecular orbitals increases as the number of atoms involved in the definition of the orbital increases and turns out to be significant in large delocalized systems, such as those defined by large transition metal clusters. For both Ni_{20} and Ni_{51} clusters different values for βs and βp, ranging between -0.1 and -3.0 have been compared. Also a different approach for the calculation of the resonant integrals, implying the geometric mean (2.2) rather than the algebraic mean (2.1), has been tested for eventual use for the study of catalytic reactions that take place on large clusters or models of surfaces.

$$\beta^{AB} = -\sqrt{(\beta^A \beta^B)} \qquad (2.2)$$

The atomic populations reported in this article are based on a Löwdin analysis. The Mulliken population analysis leads to an overpopulation of the 4s and 4p orbitals due to the observation that the maximum of these orbitals is close to the neighboring atoms, and the division of overlap population equally between the atom on which the orbital is centered and each of its neighbors is misleading. In either case, it must be recalled that any division of electrons onto individual atoms in a molecule is arbitrary, and only relative differences using the same methodologies and basis sets might have interpretive meaning.

3. Results and Discussion

The energy of the different spin states of Ni_n (n = 4, 6, 8, 13) clusters has been analyzed by means of PUHF calculations, and the results have been compared with those previously derived from ROHF-MRCI. Both methodologies lead to the same results for the smaller Ni_4 and Ni_6 clusters, but not for Ni_8 and Ni_{13}, for which large M are only obtained for the PUHF calculations. The reason for this is that the size of the CI required for these larger clusters is prohibitively expensive. This is obvious from the much lower energies that we can obtain for the UHF and PUHF calculations than we can obtain using CI methods for these larger clusters. Even so, this would not be a serious flaw if the correct magnetism could be obtained from these (relatively) small CI calculations. But on the basis of our knowledge of the large magnetic moment of bulk Ni, and the fact that it has been demonstrated that the M of the small clusters is larger than that of the bulk,[21] we have chosen PUHF calculations for the treatment of Ni_{20} and Ni_{51} tri- and bilayer slabs of (111) surfaces.

Tables 1−10 show the calculated energies for the different symmetries that have been considered for the Ni_n clusters up to the size of Ni_{13}. Odd and even table numbers correspond to ROHF and PUHF calculations, respectively.

Square planar (D_{4h}) and tetrahedral (T_d) symmetries have been evaluated for the case of Ni_4, octahedral (O_h) for Ni_6 and Ni_8, and both O_h and icosahedral (I_h) for Ni_{13}. The values shown in the tables are energies relative to the lowest, most stable states for each of the structures. Absolute energy values are also reported in the tables for comparisons.

Data in Tables 11−13 report on calculations on Ni_{20} and Ni_{51} and compare the results of the application of average and product formulas for the calculation of the resonant integrals. In these cases it is not possible to compare total energies between the two Hamiltonians—only the relative energies obtained for the given model Hamiltonian are germane.

3.1. Ni_4 Clusters. Tetrahedral and square planar structures have been studied for both the interatomic bulk distance (2.49

TABLE 1: Relative Valence Energies (Hartrees) Calculated for Ni_4 D_{4h} Structures from MRCIS Calculations[a]

M		D_{4h} 2.49 Å	D_{4h} 2.30 Å
1	energy	0.031	0.029
	state	$^1A_{1g}$	$^1A_{1g}$
3	energy	0.023	0.040
	state	^3E_u	$^3A_{1g}$
5	energy	0.025	0.036
	state	$^5B_{2g}$	$^5B_{2g}$
7	energy	0.011	0.000 (**)
	state	$^7A_{1g}$	$^7A_{1g}$
9	energy	0.000 (*)	0.003
	state	$^9A_{1g}$	$^9A_{1g}$
11	energy	0.187	0.161
	state	$^{11}A_{1g}$	$^{11}A_{1g}$

[a] Electronic states are also indicated. Different multiplicities (INDO/S MRCI) are compared for the bulk (2.49 Å) and the fully optimized geometries (INDO/1). Absolute energy values and magnetic moments per atom: (*) −162.601 hartrees, 2.236; (**) −162.842 hartrees, 1.732.

TABLE 2: Relative Valence Energies (Hartrees) Calculated for Ni_4 D_{4h} Structures from PUHF Calculations[a]

M		D_{4h} 2.49 Å	D_{4h} 2.30 Å
1	energy	0.0153	0.0160
	weight	0.2137[a]	0.2184
3	energy	0.0120	0.0127
	weight	0.5219	0.5301
5	energy	0.0024	0.0020
	weight	0.7434	0.7525
7	energy	0.0000 (*)	0.0016
	weight	0.8980	0.8993
9	energy	0.0008	0.0000 (**)
	weight	0.9963	0.9967
11	energy	0.0922	0.0980
	weight	0.9977	0.9957
13	energy	0.1904	0.2001
	weight	0.9953	0.9954

[a] Different multiplicities are compared for the bulk (2.49 Å) and the fully optimized geometries (INDO/1). Absolute energy values and calculated magnetic moments per atom: (*) −163.011 hartrees, 1.731; (**) −163.025 hartrees, 2.236. The weights are the fraction of the pure spin state contained in the UHF calculation. The projection is likely to give the most accurate description of the pure spin state after projection if this fraction is high. For example, 0.2137 indicates the original UHF calculation was 21.37% singlet. See text for further discussion of weights.

Å), and the one optimized at the ROHF level, which is close to 2.30 Å. Results of Tables 1-4 show that, at both levels of calculation, high multiplicities (*M*) characterize both symmetries.

As previously discussed in ref 19, no distortions are predicted by the ROHF/MRCI calculations for the $^7A_{1g}$ low energy state in D_{4h} symmetry. In T_d symmetry, on the other hand, the symmetry is lowered to C_{3v} through elongation along a 3-fold axis due to the nonequivalent occupation of the 3-fold degenerate t orbitals. Although the structure gains 0.18 hartrees (1 hartree = 27.211 eV = 627.5 kcal/mol) upon this distortion at the ROHF-MRCI level, it is still less stable than is the optimized D_{4h} one. C_{2v} through simultaneous elongation−compression of the T_d in perpendicular directions decreases the energy a further 0.11 hartrees to give a C_{2v} structure that appears as a distorted D_{2d} structure, but with two different neighboring Ni−Ni distances, one shorter and one longer, which is essentially isoenergetic with the D_{4h} one (−162.841 vs −162.842 hartrees).

Examining the PUHF results, Tables 2 and 4, the energy associated with the reduction of symmetry from T_d to C_{3v} is 0.065 hartrees, which is 0.101 *more* stable than the D_{4h} optimized structure. This prediction is in agreement with the

TABLE 3: Relative Valence Energies (Hartrees) Calculated for Ni_4 T_d Structures from MRCIS Calculations[a]

M		T_d 2.49 Å	T_d 2.30 Å	C_{3v}
1	energy	0.047	0.013	0.085
	state	$^1A_1$	$^1A_1$	$^1A_1$
3	energy	0.033	0.003	0.076
	state	$^3T_2$	$^3T_1$	^3E
5	energy	0.022	0.018	0.049
	state	$^5A_2$	$^5A_2$	$^5A_2$
7	energy	0.000 (*)	0.035	0.000 (***)
	state	$^7T_2$	$^7A_2$	^7E
9	energy	0.027	0.000 (**)	0.027
	state	$^9T_1$	$^9T_1$	$^9A_2$
11	energy	0.197	0.177	0.202
	state	$^{11}T_1$	$^{11}T_1$	$^{11}A_2$

[a] Electronic states are also indicated. Different multiplicities (INDO/S MRCI) are compared for the bulk (2.49 Å), the fully optimized, and the JT distorted geometries (INDO/1) associated with T_d and C_{3v} symmetries. Absolute energy values and calculated magnetic moments per atom: (*) −162.532 hartrees, 1.731; (**) −162.551 hartrees, 2.236; (***) −162.731 hartrees, 1.731.

TABLE 4: Relative Valence Energies (Hartrees) Calculated for Ni_4 T_d Structures from PUHF Calculations[a]

M		T_d 2.49 Å	T_d 2.30 Å	C_{3v}
1	energy	0.0141	0.0010	0.0141
	weight	0.2163	0.2200	0.2157
3	energy	0.0105	0.0104	0.0122
	weight	0.5305	0.5436	0.5295
5	energy	0.0033	0.0024	0.0036
	weight	0.7481	0.7611	0.7472
7	energy	0.0000 (*)	0.0000 (**)	0.0000 (***)
	weight	0.9069	0.9231	0.9061
9	energy	0.0065	0.0109	0.0061
	weight	0.9996	0.9976	0.9997
11	energy	0.1044	0.1113	0.1035
	weight	0.9955	0.9943	0.9956
13	energy	0.1904	0.2001	0.1957
	weight	0.9953	0.9954	0.9958

[a] Different multiplicities are compared for the bulk (2.49 Å), the fully optimized, and the JT distorted geometries (INDO/1) associated with T_d and C_{3v} symmetries. Absolute energy values: (*) −163.026 hartrees; (**) −163.061H; (***) −163.126 hartrees. The calculated magnetic moments per atom are 2.236.

results of most other calculations. The C_{2v} structure described above leads to a slightly more stable structure. We note that the PUHF calculations have lower energies, ranging from 0.3 to 0.5 hartrees, than the MR/CIS calculations, and on this ground might be considered the more reliable.

In all the cases (symmetries and calculation procedures) states of $M = 7$ and 9 are competing for the lowest energy. The competing states are predicted to lie closer in energy at the PUHF than at the ROHF-MRCI level. In addition, the PUHF results seem more consistent with a Heisenberg spin Hamiltonian fitted to these results, and the total energies obtained through the PUHF calculations are lower than those we are able to obtain with the limited MRCI we can afford to perform.

For the D_{4h} and T_d symmetries with bulklike distances MRCI calculations stabilize states of $M = 9$ and 7, respectively, although states of $M = 5$, 7, and 9 are close in energy for the latter. For the optimized geometry (Tables 1 and 3) an *M* value of 7 is preferred. At the PUHF level, states of $M = 7$ and $M = 9$ in D_{4h} symmetry differ in only 0.5 and 1.0 kcal/mol for the bulk and optimized interatomic distances, respectively (Table 2). The structure of $M = 9$ gives, in both cases, better convergence in the spin density with no distortion predicted. States of $M = 5$ are also close in energy to the septets and nonets for the bulklike and optimized T_d structures according

TABLE 5: Relative Valence Energies (Hartrees) Calculated for Ni_6 Structures from MRCIS Calculations[a]

M		O_h 2.49 Å	O_h 2.36 Å	D_{4h}
1	energy	0.170	0.104	0.118
	state	$^1A_{2g}$	$^1A_{2g}$	$^1B_{1g}$
3	energy	0.116	0.045	0.063
	state	$^3T_{2u}$	$^3T_{2u}$	$^3B_{2u}$
5	energy	0.102	0.040	0.029
	state	$^5A_{2g}$	$^5A_{2g}$	$^5B_{1g}$
7	energy	0.035	0.042	0.041
	state	$^7A_{2g}$	$^7A_{2g}$	$^7B^{1g}$
9	energy	0.011	0.011	0.025
	state	$^9A_{2g}$	$^9A_{2g}$	$^9B_{1g}$
11	energy	0.000 (*)	0.000 (**)	0.000 (***)
	state	$^{11}E_g$	$^{11}E_g$	$^{11}A_{1g}$
13	energy	0.020	0.043	0.063
	state	$^{13}A_{2g}$	$^{13}E_g$	$^{13}B_{1g}$

[a] Electronic states are also indicated. Different multiplicities (INDO/S MRCI) are compared for the bulk (2.49 Å), the fully optimized, and the JT distorted geometries (INDO/1) associated with O_h and D_{4h} symmetries. Absolute energy values: (*) −244.224 hartrees; (**) −244.295 hartrees; (***) −244.300 hartrees. The calculated magnetic moment per atom is 1.825 μ_B.

TABLE 6: Relative Valence Energies (Hartrees) Calculated for Ni_6 Structures from PUHF Calculations[a]

M		O_h 2.49 Å	O_h 2.36 Å	D_{4h}
1	energy	0.018	0.023	0.0096
	weight	0.1579	0.1604	0.1597
3	energy	0.021	0.0116	0.0135
	weight	0.4065	0.4091	0.4078
5	energy	0.010	0.005	0.0085
	weight	0.5890	0.5965	0.5996
7	energy	0.0035	0.001	0.0011
	weight	0.7358	0.7466	0.7475
9	energy	0.0011	0.0003	0.00015
	weight	0.8537	0.8630	0.8646
11	energy	0.000 (*)	0.000 (**)	0.000 (***)
	weight	0.9517	0.9628	0.9634
13	energy	0.014	0.021	0.0187
	weight	0.9994	0.9955	0.9969

[a] Different multiplicities are compared for the bulk (2.49 Å), the fully optimized, and the JT distorted geometries (INDO/1) associated with O_h and D_{4h} symmetries. Absolute energy values: (*) −244.725 hartrees. The calculated magnetic moments per atom are 1.525.

TABLE 7: Relative Valence Energies (Hartrees) Calculated for Ni_8 Structures from MRCIS Calculations[a]

M		O_h 2.49 Å	O_h 2.25 Å	O_h 2.15 Å
1	energy	0.000 (*)	0.032	0.030
	state	$^1A_{1g}$	$^1T_{2u}$	$^1T_{2u}$
3	energy	0.018	0.000 (**)	0.000 (***)
	state	^3E_u	$^3T_{2u}$	$^3T_{2u}$
5	energy	0.098	0.033	0.006
	state	$^5A_{1g}$	^5E_g	$^5A_{1g}$
7	energy	0.139	0.076	0.016
	state	$^7A_{1g}$	$^7T_{1u}$	$^7A_{1g}$
9	energy	0.186	0.123	0.029
	state	$^9A_{1u}$	$^9T_{2g}$	$^9A_{1u}$

[a] Electronic states are also indicated. Different multiplicities (INDO/S MRCI) are compared for the bulk (2.49 Å), the fully optimized INDO/1 (2.25 Å), and the geometry that result from the DFT calculations of R&K. Absolute energy values: (*) −325.2382 hartrees; (**) −325.3797 hartrees; (***) −325.2449 hartrees.

to PUHF calculations (1.8 and 1.5 kcal/mol respectively) (Table 4). The convergence pattern in the spin density (the fit to the Heisenberg model) indicates that a state on $M = 5$ would be the most stable as a regular T_d, whereas a C_{3v} distortion slightly favors $M = 7$ over $M = 5$, a prediction that is in agreement with the results of the MRCI calculations.

TABLE 8: Relative Valence Energies (Hartrees) Calculated for Ni_8 Structures from PUHF Calculations[a]

M		O_h 2.49 Å	O_h 2.25 Å	O_h 2.15 Å
1	energy	0.0184	0.0178	0.0361
	weight	0.1194	0.1251	0.1266
3	energy	0.0252	0.0271	0.0324
	weight	0.3216	0.3321	0.3387
5	energy	0.0215	0.0258	0.0203
	weight	0.4828	0.4974	0.5041
7	energy	0.0110	0.0114	0.0214
	weight	0.6197	0.6330	0.6359
9	energy	0.0059	0.0060	0.0000 (***)
	weight	0.7304	0.7410	0.7619
11	energy	0.0029	0.0000 (**)	0.0028
	weight	0.8206	0.8338	0.8394
13	energy	0.0000 (*)	0.0048	0.0061
	weight	0.8986	0.9013	0.9150
15	energy	0.0057	0.0083	0.0101
	weight	0.9599	0.9610	0.9680

[a] Different multiplicities (INDO/S MRCI) are compared for the bulk (2.49 Å), the fully optimized (2.25 Å), and the geometry that result from the DFT calculations of R&K. Absolute energy values and calculated magnetic moments per atom: (*) −326.3154 hartrees, 1.62; (**) −326.1830 hartrees, 1.371; (***) −325.6042 hartrees, 1.118.

TABLE 9: Total Valence Energies (Hartrees) Calculated for Ni_{13} Structures from MRCIS Calculations[a]

M		I_h 2.49 Å	O_h 2.41 Å
1	energy	0.0005	0.0000 (**)
	state	$^1T_{1g}$	$^1A_{1g}$
3	energy	0.0000 (*)	0.0023
	state	$^3T_{1g}$	$^3T_{2g}$
5	energy	0.0942	0.0934
	state	^5H_u	$^5A_{2u}$
7	energy	0.1879	0.1483
	state	^7H_u	$^7A_{2u}$
9	energy	0.2819	0.2202
	state	$^9T_{2u}$	^9E_u

[a] Electronic states are also indicated. Different multiplicities (INDO/S MRCI) are compared for the I_h and O_h symmetries. Absolute energy values: (*) −529.6527 hartrees; (**) −529.9689 hartrees.

TABLE 10: Relative Valence Energies (Hartrees) Calculated for Ni_{13} Structures from PUHF Calculations[a]

M		I_h 2.49 Å	O_h 2.49 Å	O_h 2.41 Å
1	energy	0.1344	0.0408	0.0096
	weight	0.3986	0.0782	0.0792
3	energy	0.0351	0.0225	0.0245
	weight	0.2255	0.2185	0.2199
5	energy	0.0161	0.0258	0.0241
	weight	0.3745	0.3428	0.3474
7	energy	0.0162	0.00097	0.0092
	weight	0.4830	0.4439	0.4540
9	energy	0.0081	0.0000 (**)	0.0000 (***)
	weight	0.5859	0.5352	0.5384
11	energy	0.0000 (*)	0.0087	0.0065
	weight	0.6715	0.6150	0.6157
13	energy	0.0057	0.0098	0.0111
	weight	0.7202	0.6980	0.6871

[a] Different multiplicities (INDO/S MRCI) are compared for the bulk (2.49 Å) and the fully optimized INDO/1 geometry for both the I_h and O_h symmetries. Absolute energy values and calculated magnetic moments per atom: (*) −535.6252 hartrees, 0.843; (**) −533.9870 hartrees, 0.688; (***) −533.7668 hartrees, 0.688.

The small energy differences between the states of $M = 7$ and $M = 9$ and the predicted JT distortion by both approaches demonstrate the consistency of these methods for this cluster. These results might be compared with those obtained from the density functional calculations of Reuse and Khanna (R&K),[22] which, using the local density approximation (LDA) and their

TABLE 11: PUHF Relative Valence Energies (Hartrees) Calculated for Ni_{20} Surface Slabs Modeled with the Interatomic Distances of the Bulk[a]

M		Bk 2.49 Å	*M*		Bk 2.49 Å
1	energy	0.0149	11	energy	0.0020
	weight	0.0525		weight	0.4685
3	energy	0.0147	13	energy	0.0006
	weight	0.1412		weight	0.5712
5	energy	0.0142	15	energy	0.0000
	weight	0.2071		weight	0.5927
7	energy	0.0145	17	energy	0.0028
	weight	0.3317		weight	0.6231
9	energy	0.0042	19	energy	0.0064
	weight	0.4735		weight	0.6637

[a] $M = 2S + 1$. The calculations reported here use the sum formula for the resonance integral β. Comparisons with the product formula are discussed in the text.

TABLE 12: UHF and PUHF Valence Energies (Hartrees) for the Most Stable Calculated *M* of Ni_{51} Surface Slabs, Using the Average Formula for the Resonant Integrals[a]

M/μ (μ_b)	*E* UHF	*E* PUHF	*S*	weight
29/0.569	−2790.2080	−2790.2028	14	0.43
		−2790.2070	15	0.25
		−2790.2131	16	0.15
31/0.607	−2790.2204	−2790.2148	15	0.46
		−2790.2198	16	0.26
		−2790.2250	17	0.14
33/0.647	−2790.1989	−2790.1940	16	0.47
		−2790.1979	17	0.26
		−2790.2018	18	0.14
35/0.686	−2790.1674	−2790.1634	17	0.48
		−2790.1673	18	0.26
		−2790.1714	19	0.13
37/0.725	−2790.1057	−2790.1020	18	0.50
		−2790.1058	19	0.26
		−2790.1097	20	0.13
39/0.765	−2790.1499	−2790.1497	19	0.52
		−2790.1503	20	0.26
		−2790.1227	21	0.12

[a] μ = magnetic moment per atom.

TABLE 13: UHF and PUHF Valence Energies (Hartrees) for the Most Stable Calculated *M* of Ni_{51} Surface Slabs, Using the Product Formula in the Calculation of the Beta Values[a]

M/μ (μ_b)	*E* UHF	*E* PUHF	*S*	weight
33/0.647	−2794.3989	−2794.3998	16	0.723
		−2794.3979	17	0.209
		−2794.3956	18	0.055
37/0.725	−2794.4610	−2794.4617	18	0.802
		−2794.4590	19	0.163
		−2794.4551	20	0.028
39/0.764	−2794.4757	−2794.4762	19	0.843
		−2794.4734	20	0.136
		−2794.4697	21	0.018
41/0.801t	−2794.4795	−2794.4801	20	0.867
		−2794.4767	21	0.118
		−2794.4721	22	0.013
43/0.842	−2794.4661	−2794.4667	21	0.872
		−2794.4630	22	0.114
		−2794.4578	23	0.123

[a] The total energies here should not be compared with those reported in Table 12, as they refer to calculations using a different Hamiltonian; see text.

own Gaussian implementation, show that square planar and distorted T_d (D_{2d}) structures of $M = 7$ are competing for the definition of the ground state (GS) of Ni_4. Nonlocal DFT calculations by Castro, Jamorski, and Salahub,[7] suggest that a distorted T_d structure (D_{2d}), this time with $M = 5$, is the most stable. This result was supported by more recent calculations of Cisneros, Castro and Salahub,[46b] who, at both the LSD and GGA levels, found the septet located 0.85 and 0.61 eV higher in energy, respectively, and the nonet located 1.94 and 2.05 eV, respectively, above the GS. A distorted T_d geometry with $M = 5$ is also predicted as most stable by the more recent calculations of Michelini et al.[42] The similarity of the results of Castro et al. and Michelini et al. is a consequence of the similarity of the procedures.

The previous discussion shows that when an INDO/S model is applied to the study of Ni_4 clusters, the PUHF and MR/CIS calculations favor the same *M*, although the differences in energy between different *M* are often quite small. The PUHF model suggests that the distorted T_d structure lies lowest in energy, whereas the MR/CIS predicts the two structures essentially degenerate. DFT calculations predict the distorted T_d structure to lie lowest. Since spin polarized DFT and the UHF Hartree−Fock calculations are similar in the way they treat spins, the coincidence of the PUHF and DFT results of R&K might suggest that the contamination of higher spin components in the DFT calculation are not important, at least for the smaller clusters. Comparing our results with those of Castro et al., we remark that we optimize the different clusters confined to a given symmetry, as previously described.[19] Distortions are modeled from these higher symmetry structures and then further optimized using gradient techniques to avoid spurious JT distortions that result from symmetry breaking during the SCF cycles. We have found that, within HF methodologies, other procedures often lead to spurious distortions of the symmetry.

3.2. Ni_6 Clusters. O_h structures have been studied for both the interatomic bulk distance and the one optimized to minimum energy.

An $^{11}E_g$ state is calculated as the most stable by means of MRCI calculations (Table 5), for both the bulklike and the optimized geometry. States of $M = 9$ are 6.8 kcal/mol higher in energy. The optimized O_h cluster JT distorts, by means of an axial elongation, breaking the degeneracy of the half-filled e_g orbital. The distorted structure is calculated to be 3.0 kcal/mol more stable than the optimized O_h one and also prefers $M = 11$.

According to the PUHF calculations, states of $M = 9$ and $M = 11$ are within less than 1 kcal/mol for the bulklike structure (Table 6). The energy differences are even smaller for the optimized ones. The spin density distribution indicates that a JT distortion along the *z* axis would stabilize the system. The distorted structure is well convergent for states of $M = 7$, 9, 11, which are within 1 kcal/mol, with the last one most stable. It is unlikely that the INDO Hamiltonian is reliable to within 1 kcal/mol.

The results for this cluster size can be compared with those derived from the ab initio CASSCF calculations by Gropen and Almlöf (G&A)[20] and from the DFT calculations by R&K.[22] CASSCF calculations have been performed only for the bulklike structure, with no geometry optimization. A state of $M = 7$ was found, and no distortion was analyzed. However, in relation to these data, it is noteworthy that, for a given electronic configuration, G&A calculated the unusual result of a septet more stable than the nonet. DFT calculations by R&K also show minimal distortions from an O_h symmetry for Ni_6. Although high multiplicities are also stabilized, both the optimized distance and the calculated multiplicities ($M = 9$) are somewhat smaller than ours. Recent experiments suggest that the ground state of Ni_6 is a nonet.[43]

As in the case of Ni_4, the fact that the structures are characterized by high M is well described by both levels of theory. In this case, PUHF calculations seem the more successful in describing the stability of the nonet, which seems to be supported by the experimental results.

3.3. Ni_8 Clusters. O_h symmetries have been also analyzed for this cluster size. To compare the results with those derived by other authors, using different methodologies, not only the interatomic distance and the one optimized to minimum energy within our ROHF approach have been considered but also the one that results from DFT calculations.[22]

Following the same scheme previously described, PUHF and ROHF-MRCI calculations have been compared in the description of the spin states of the different structures. The results from both methodologies suggest that M is strongly distance dependent (Tables 7 and 8). However, whereas M decreases when the distances in the cluster increase in the ROHF approach, the reverse trend is followed in the PUHF calculations. Increased M with increased distance might be expected as the Ni atom itself is triplet. The failure of the ROHF-MRCI calculation to follow this trend is a ramification of our inability to perform a large enough CI to restore the atomic-like nature to the constituent atoms in this size cluster. This can be seen by examining the total energies given in Tables 7 and 8 in the footnotes. At 2.05 Å this difference is only 0.36 hartrees, while at the 2.49 Å distance the difference is 1.08 hartrees, with the PUHF calculations always lower. In the limit of full CI the ROHF-CI calculations would be lower. In the PUHF calculations, the effect is correctly reproduced through a more proper treatment of the exchange in the zeroth-order wave function, but this treatment actually exaggerates this effect and favors larger intermolecular distances. This is also quite clear from the total energies reported for both treatments.

The ROHF-MRCI methodologies favor a $^1A_{1g}$ state for the bulklike structure, and a $^3T_{2u}$ state for the optimized one. M values larger than 9 are preferred by PUHF calculations. $M = 13$, $M = 11$, and $M = 9$ are stabilized for $r = 2.49$, 2.25, and 2.05 Å, respectively, but the values are within 3.75 kcal/mol in the three cases.

From the nonequivalent filling of degenerate orbitals, symmetry breaking was predicted by the MRCI calculations in all the cases but the one that mimics the bulk, which is associated with $M = 1$.[19] The spin density distribution that results from the PUHF calculations suggests distortions of the O_h to structures of D_{2h} symmetry, which result from an elongation along a diagonal axis followed by compression of the squared faces along an axis perpendicular to it.

Only the results from R&K,[22] which supports $M = 9$, are available for comparison within O_h symmetry. From our previous description, the similarity between the DFT and PUHF results becomes evident. The same M value is predicted by both methodologies for a given cluster size. No distortion of the O_h symmetry were considered in the DFT calculations of R&K.

We have not analyzed other symmetries because we are interested in the structures that more closely resembles a piece of the bulk for each cluster size. Recent theoretical studies by Desmarais, Jamorski, Reuse, and Khanna,[21] on the geometry and magnetic moments of Ni_8 clusters, have found a D_2 bisdisphenoid GS of $M = 9$. Although dealing with a different symmetry, this result is also in agreement with our PUHF calculated magnetism. This coincidence might lend support to the observation made in ref 21 that, for a given number of atoms, structures with a different coordination of atoms have the same M.

Our calculated ionization potential of 6.87 eV is also in good agreement with the 6.71 eV value reported in ref 21. Both are higher than the experimental value of 6.13 eV.[43] A possible explanation is based on the fact that the comparison involves calculated vertical ionization potentials and experimentally measured adiabatic ones.

3.4. Ni_{13} Clusters. The same methodologies have been compared for the description of Ni_{13} clusters. Within the INDO/1 approach, optimization of the geometry leads to structures characterized by the interatomic bulk distance in the case of a perfect I_h, and by a value that is only 0.07 Å smaller in O_h symmetry. When ROHF-MRCI and PUHF methodologies are applied for the study of the electronic and magnetic properties (M) of these optimized structures, in the framework of the INDO/S approach, the conclusions previously discussed for Ni_8 are reconfirmed.

Very low M values, associated with $^1A_{1g}$ and $^3T_{1g}$ are favored for the I_h and O_h symmetries, respectively, at the MRCI level, with the singlets and the triplets almost degenerate in both cases (Table 9). Even when 35 reference states and 2500 configurations are used in the calculations, the size of the CI is not large enough to reproduce the correct order of spin multiplicities. As seen previously, the PUHF energies are very much lower, and we are forced to either increase the size of the CI, which we are presently examining, or abandon the use of this procedure on the larger clusters on which we wish to examine chemistry. This is a general conclusion: in open-shell systems such as these it is difficult to obtain an energy using ROHF/CI procedures that is competitive with that obtained from the far simpler UHF method. This is somewhat inconsistent in the sense that the better geometries are obtained through the ROHF-CI procedure—the PUHF procedure favors larger Ni−Ni distances, but generally has the lower total energy. This is not unlike the situation already observed in transition metal dimers.[29]

PUHF calculations stabilize large M values (Table 10). An undectet is predicted in I_h symmetry, which is 3.2 kcal/mol more stable than the state of $M = 13$, and 5.1 kcal more stable than the nonet. This result is in agreement with recent magnetic evidence that suggest that Ni_{13} is an undectet.[16] The O_h structure has been analyzed for two, very close situations related to the bulk and optimized geometry. $M = 9$ is favored in both of these O_h cases, with states of $M = 7$ and $M = 11$ within 6 kcal/mol. An elongation of the O_h structure is also predicted. No data for this symmetry are available for comparison in the related literature. According to the PUHF calculations it is, on the other hand, less stable than the I_h.

The results of R&K,[22] which are the only data available for comparison, predict a GS of $M = 9$ in I_h symmetry, with the states of $M = 11$ and $M = 13$ marginally above it. Nothing is said in ref 22 about the O_h symmetry.

Whereas no distortions are analyzed in the DFT calculations, the spin density distribution that results from the PUHF calculations indicates that an elongation of the I_h structure might be considered.

3.5. Ni(111) Surface Slab Model Clusters. As an example of the power of the PUHF procedure we examine pieces of the [111] surface, modeling this with trilayer slabs of 20 and bilayer slabs of 51 Ni atoms. These particular pieces of solid are unlikely to exist other than as a model of the [111] surface, as they would likely rearrange geometrically to a more spherical form.

For these particular models, different parametrizations of the resonant integrals have been tested. These different parametrizations include both the use of the algebraic or geometric

averages for the calculation of β^{AB}, as discussed previously, as well as different β values for the s and p orbitals in each case, ranging from -0.1 to -3.0. We found the results more dependent on the parametrization as the size of the cluster increases; as the accumulation of errors becomes more apparent as the number of interactions between the atomic orbitals increases.

3.5.1. Ni_{20} Clusters. Calculations on Ni_{20} using the standard default parametrization of ZINDO/S lead to the results shown in Table 11. This standard parametrization implies the use of the average formula, for $\beta s = \beta p = -1.0$ eV and $\beta d = -32.0$ eV.

The projected UHF calculations present no difficulty converging for any of the multiplicities. We found a GS of $M = 15$, which is only 1.3 kcal/mol more stable than the states of $M = 11$ and $M = 13$. States of $M = 9$ are only 2.6 kcal/mol far from the quindectet. The calculated magnetic moment, 0.748 μ_B/Ni atom, is closer but still does not reproduces the magnetic behavior of the bulk metal of 0.6. The electronic distribution is described by a population close to $d^{8.5}s^{1.5}$ on each Ni atom. This description is not dependent on the value assigned to the atomic β's.

The HOMO is 4s in character. Within the Koopmanns approximation we calculate an ionization potential of 6.74 eV, reasonably close to the experimental value of 5.82 eV.[43]

When the product formula is applied, different values of βs and βp between -0.1 and -3.0 eV, do not change the calculated *M*, but the values of the IP closest to the experimental ones are reproduced with $\beta s = \beta p = -3.0$ eV. For this set of parameters, states of $M = 11$, $M = 13$, and $M = 15$ are within 2.8 kcal/mol, with the undectet the most stable. The calculated magnetic moment for this trilayer model system (0.55) is very close to the experimental value for the bulk metal. The atomic population, on the other hand, is close to d^9s^1 on each atomic center. The calculated IP (5.15 eV) is closer to the experimental value than the one that results from the application of the average formula.

We have found no theoretical data in the related literature to be compared with ours.

3.5.2. Ni_{51} Clusters. Calculations on Ni_{51} are of great interest for both catalysis and theoretical research. There is little question that clusters of this size begin to resemble the bulk.

When the standard parametrization is used, states of $M = 1$ are easily convergent at the UHF level, but the analysis of higher *M* is not straightforward. The eigenvectors that converge for $M = 1$ evolve to a different wave function for higher *M* values.

According to the UHF calculations, a state of $M = 31$ ($M = 0.607$ μ_B) is the most stable. However, after projection of the high-spin components, $M = 35$ is predicted. Table 12 shows this effect, together with the calculated magnetic moments for the most stable multiplicities, which are close to the experimental value for the bulk metal (0.606 μ_B). The results of the calculations are unusual in the sense that, after projection of the initial UHF wave function the total energy does not decrease, and states of higher *M* are favored. They are also unusual in the larger differences observed between the energies of the various states after projection.[41] This suggests that there are very many states in this region of energy, and the PUHF procedure is sampling them. This is not surprising.

When calculations are performed using initial vectors from the $M = 1$ calculation, a wave function of a clearly different nature is obtained, which stabilizes states of $M = 5$ at the PUHF level. They are, on the other hand, about 1.5 hartrees higher in energy than the ones associated with large *M*. In addition to its higher energy, the calculated magnetic moment does not describe the magnetic behavior of bulk Ni.

There is no symmetry breaking in the wave functions, neither in the one associated with large magnetic moments nor in the one related to low *M* values.

Whereas the HOMO is 4s in character in both cases, the population on each Ni atom is d^8s^2 in the first case and d^9s^1 in the second. It is well-known that many of the difficulties found in the theoretical treatment of Ni clusters originate from the near degeneracy of d^8s^2 and d^9s^1 states of the atom itself—even the terms arising from these two configurations are interspersed. Our UHF calculations on Ni_{51} are a clear example of this effect.

We found that this behavior does not depend on the value of the resonance integral assumed in the calculation.

Although an accurate description of the magnetic behavior of Ni_{51} clusters is achieved with the average formula, the calculated IP is about 4 eV larger than the one experimentally measured.[44]

Use of the product formula in the calculation of the resonant integrals helps to overcome this problem (Table 13). Using this model, the same set of molecular orbitals are capable of describing states of *M* ranging from $M = 1$ to $M = 43$. The MOs are characterized by a population on the s orbitals of the atomic centers that varies from 0.5 on the edge atoms to 0.7 on the atoms in the center.

When the product formula is used, the most stable state is calculated for $M = 41$ (Table 13). States of $M = 43$ to $M = 39$ are within 2.3 kcal/mol of it.

The stability of the wave function for the description of the states of different *M*, and the behavior of the wave function after projection, which show small spin contamination by higher spin components, are indicative of a more convergent description of the electronic structure of this metallic cluster using this model than that obtained using the algebraic mean for the resonance term. Projection of higher multiplicities from the UHF function lowers the energy in each case, and predictions are similar. For example, the energy of the $M = 41$ ($S = 20$) state after projection, -2794.4801 hartrees, is very similar to that obtained for the $M = 39$ UHF function $S = 20$ state of -2794.4734 hartrees, a difference of 0.0067 hartrees = 0.18 eV for two very different calculations.[41] We note that it is not possible to compare the total energies of Tables 12 and 13, as they refer to different Hamiltonians: only the relative energies within the same Hamiltonian (table in this case) can be compared.

The HOMO is 4s in character, leading to a calculated IP of 5.05 eV, which is reasonably close to the experimental value of 5.8 eV,[43] but the unknown experimental structure is likely not that which we have modeled here. The value for the bulk is estimated at 5.5 eV.

The predicted magnetic moment (0.80) is still larger than the one of the bulk. It is in agreement, however, with the experimental data for clusters larger than 50 atoms.[43] From the comparison of Ni_{20} and Ni_{51} clusters it might be concluded that the trilayer structures are necessary to achieve a spin pairing capable of modeling the magnetism of bulk Ni.

4. Conclusions

We have examined the ability of two quantum chemical models to evaluate magnetic properties of TM clusters using Ni as a test species. Within a semiempirical INDO/S approach, PUHF and ROHF-MRCI calculations lead to similar results for

clusters in size up to the O_h Ni_6. For clusters larger than this, the size of the CI for an appropriate accuracy, or consistency, becomes prohibitive, a fact that poses the question of whether such calculations will really be of practical value in modeling catalytic processes on surfaces. For cluster sizes larger than the hexamer, PUHF and the available DFT calculations agree well. Our confidence in the large M values that such calculations favor is further supported by the values of the magnetic moment per atom calculated for the large clusters, which, for trilayer slab models, reproduces the value of the bulk.

When PUHF and DFT calculations are compared, it is found that, at any level of calculation, high M are predicted for the small clusters, up to Ni_{13}. Looking at the energy differences between the most stable states for a given cluster size, associated with different M, the question remains open of whether the small differences among the calculated values are not consequences of the parametrization, selected model potentials, or even the accuracy of the calculations. There is no doubt, however, that when the applied methodology is disregarded, the predicted M for small clusters is larger than the one that characterizes bulk metal.

This article is one of the few that examine the electronic structure of large clusters, choosing Ni_{20} and Ni_{51} surface slabs as models for bulk Ni. LCGTO-LDF calculations by Pacchioni and Rösch on O_h Ni clusters, have found magnetic moments between 0.72 and 0.79 μ_B for 44 and 19 atom clusters built up on the interatomic bulk distance.[45,46] Although the calculated moments are close to ours, the small discrepancies, when the values derived from the product formula are considered, might well originate from the different coordination numbers of the structures under comparison. The average coordination number in the O_h Ni_{19} structure[45,46] is smaller than that in the trilayer Ni_{20} surface magnetism. A similar comparison applied to the O_h Ni_{44} and the bilayer Ni_{51} surface cluster explains the larger magnetic moment calculated for the latter.

According to the super-paramagnetic theory[47] and the experimentally measured magnetic moments, values larger than those of the bulk, ranging from 0.8 to 1.0 μ_B, are expected for Ni clusters with sizes close to 50 atoms. Although this value refers to nanometric particles of minimized geometry instead of models of a (111) surface, they agree with our prediction for Ni_{51}.

This research is eventually targeted to examine adsorption studies, focusing on systems of importance in heterogeneous catalysis, which needs an accurate definition of the spin states for the initial naked structures as well as for the final adsorbed systems. The use of the product formula in the calculation of β^{AB} has not been examined in great detail for many systems, whereas the sum average has now been used in thousands of examples. In those cases where β^A and β^B are similar, the product and sum averages will give quite similar results, made even more similar by adjustments of the β values in the product form. On the other hand, when the values are very different, as they are for s and d interaction on Ni, the $\beta_{sd}{}^{AB}$ are different. This difference is not very apparent in transition metal complexes in which, in general, the metal 4s and 4p orbitals have little role to play, because they are either emptied in the formation of the positive ion or destabilized by covalent bonding, or both. This is not the case in these large clusters. Similar observations have been made in the study of LiF clusters, in which, again, there is a large difference between the β^{Li} and β^F parameters, and there are many such interactions.[48] The geometric average form will need to be carefully evaluated in the context of all the atoms that are presently parametrized within this model, and that is a formidable task.

The comparative analysis presented in this article, which has been aimed at finding the best way of dealing with the open shell distribution of TM clusters, shows that PUHF calculations define a computationally easier approach, one that seems capable of successfully describing the magnetic properties of the TM clusters we have examined in this study.

Acknowledgment. This work was supported in part through grants from the Office of Naval Research and the Consejo Nacional de Investigaciones Cientificas y Tecnicas (CONICET), Republica Argentina, and the University of La Plata. Most of these calculations were aided through a SUR grant from the IBM Corp.

References and Notes

(1) Jacobs, P. W.; Wind, S. J.; Ribeiro, F. H.; Somorjai, G. A. *Surf. Sci.* **1997**, *372*, L249.
(2) Forni, A.; Tartadini, G. F. *Surf. Sci.* **1996**, *352*−*354*, 142.
(3) Paul, J. F.; Sautet, P. *Surf. Sci.* **1996**, *356*, L 403.
(4) Rodriguez, A.; Amiens, C.; Chaudret, B.; Casanove, M. J.; Lecante, P.; Bradley, J. S. *Chem. Mater.* **1996**, *8*, 1978.
(5) Galan, F.; Fouassier, M.; Tranquille, M.; Mascetti, J.; Papai, I. *J. Phys. Chem A* **1997**, *101*, 2626.
(6) Delbecq, F.; Moraweck, B.; Verite, L. *Surf. Sci.* **1998**, *396*, 156.
(7) (a) Castro, M.; Jamorski, C.; Salahub, D. R. *Chem. Phys. Lett.* **1997**, *271*, 133. (b) Cisneros, A.; Castro, M.; Salahub, D. *Int. J. Quantum Chem.*, submitted.
(8) Klabunde, K. J. *Free Atoms, Clusters, and Nanoscale Particles*; Academic Press: San Diego, 1994.
(9) Perkins, L. S.; DePristo, A. E. *Surf. Sci.* **1994**, *317*, L1152.
(10) Fujima, N.; Yamaguchi, T. *J. Phys. Soc. Jpn.* **1989**, *58*, 1334.
(11) Gunter, P. L. J.; Niemantsverdriet, J. W.; Ribeiro, F. H.; Somorjai, G. A. *Catal. Rev.*−*Sci. Eng.* **1997**, *39* (1&2), 77.
(12) Tolman, W. *Acc. Chem. Res.* **1998**, *30*, 227.
(13) Sono, M.; Roach, M. P.; Coulter, E. D.; Dawson, J. H. *Chem. Rev.* **1996**, *96*, 2841.
(14) Spiro, T. G. *Iron*−*Sulfur Proteins*; Wiley: New York, 1982.
(15) Nayak, S. K.; Khanna, S. N.; Rao, B. K.; Jena, P. *J. Phys. Chem. A* **1997**, *101*, 1072.
(16) Parks, E. K.; Zhu, L.; Ho, J.; Riley, S. J. *J. Chem. Phys.* **1994**, *100*, 7206; *J. Chem. Phys.* **1995**, *102*, 7377. Parks, E. K.; Riley, S. J. *Z. Phys. D* **1995**, *33*, 59.
(17) Behm, J. M.; Arrington, C. A.; Morse, M. D. *J. Chem. Phys.* **1993**, *99*, 6409.
(18) Yang, D. S.; Zgierski, M. Z.; Bercés, A.; Hackett, P. A.; Roy, P. N.; Martinez, A.; Carrington, T.; Salahub, D. R.; Fournier, R.; Pang, T.; Chen. C. *J. Chem. Phys.* **1996**, *105*, 10663.
(19) Estiú, G. L.; Zerner, M. C. *J. Phys. Chem.* **1996**, *100*, 16874.
(20) Gropen, O.; Almlöf, J. *Chem. Phys. Lett.* **1992**, *191*, 306.
(21) Desmarais, N.; Jamorski, C.; Reuse, F. A.; Khanna, S. N. *Chem. Phys. Lett.* **1998**, *294*, 480.
(22) Reuse, F. A.; Khanna, S. N. *Chem. Phys. Lett.* **1995**, *234*, 77.
(23) Nayak, S. K.; Rao, B. K.; Khanna, S. N.; Jena, P. *Chem. Phys. Lett.* **1996**, *259*, 588.
(24) Nayak, S. K.; Reddy, B.; Rao, B. K.; Khanna, S. N.; Jena, P. *Chem. Phys. Lett.* **1996**, *253*, 390.
(25) Jamorski, C.; Martinez, A.; Castro, M.; Salahub, D. R. *Phys. Rev. B* **1997**, *55*, 10905.
(26) Calaminici, P.; Koster, A. M.; Russo, N.; Salahub, D. R. *J. Chem. Phys.* **1996**, *105*, 9546.
(27) Wetzel, T. L.; DePristo, A. E. *J. Chem. Phys.* **1996**, *105*, 572.
(28) M. Dupuis presented, at the 1997 Sanibel Symposia, St. Agustine, FL, evidence that DFT predicts low spin in Fe(III) prophyrin systems when compared to highly correlated ab initio calculations, INDO/s calculations, and experiment. It is, however, not possible to generalize these results, because of the variety of functionals that might be used in the former case and the size of the CI calculations in the latter cases.
(29) (a) Szabo, A.; Ostlund, N. *Modern Quantum Chemistry*, 1st ed.; Macmillian Press: New York, 1982. (b) Martin, C.; Zerner, M. C. Electronic Structure Calculations on Transition Metal Complexes: Ab Initio and Approximate Models. In *Inorganic Electronic Structure and Spectroscopy*; Lever, B., Solomon, E., Eds.; J. Wiley and Sons: New York, 1999.
(30) Pople, J. A.; Nesbet, R. K. *J. Chem. Phys.* **1954**, *22*, 571.
(31) Zerner, M. C. *Int. J. Quantum Chem.* **1989**, *35*, 567.

(32) Edwards, W. D.; Zerner, M. C. *Theor. Chim. Acta* **1987**, *72*, 347.
(33) Pauncz, R. *Spin Eigenfunctions*; Plenum Press: New York, 1979.
(34) Zerner, M. C. ZINDO. Quantum Theory Project; University of Florida, Gainesville.
(35) Zerner, M. C. In *Reviews in Computational Chemistry*; Lipkowitz, K. B., Boyd, B., Eds.; VCH Publishers: New York, 1990; Vol 2.
(36) Ridley, J.; Zerner, M. C. *Theor. Chim. Acta* **1973**, *32*, 111.
(37) Zerner, M. C.; Loew, G. H.; Kirchner, R. F.; Mueller-Westerhoff, U. T. *J. Am. Chem. Soc.* **1980**, *102*, 589.
(38) Bacon, A. D.; Zerner, M. C. *Theor. Chim Acta* **1979**, *53*, 21.
(39) *CRC Handbook*; CRC Press; Boca Raton, FL.
(40) Harriman, J. F. *J. Chem. Phys.* **1964**, *40*, 2827.
(41) Cory, M. G.; Zerner, M. C. *J. Phys. Chem.* **1999**, *103*, 7287.
(42) Michelini, M. C.; Pis-Diez, R.; Jubert, A. *Int. J. Quantum Chem.*, to be submitted.
(43) Apsel, S. E.; Emmert, J. W.; Deng, J.; Bloomfield, L. A. *Phys. Rev. Lett.* **1996**, *76*, 1441.
(44) Knickelbein, M. B.; Yang, S.; Riley, S. J. *J. Chem. Phys.* **1990**, *93*, 94.
(45) Rösch, N.; Ackermann, L.; Pacchioni, G. *Chem. Phys. Lett.* **1992**, *199*, 275.
(46) Pacchioni, G.; Rösch, N. *Acc. Chem. Res.* **1995**, *28*, 390.
(47) (a) Fujima, N.; Yamaguchi, T. *Phys. Rev. B* **1996**, *54*, 26. (b) Fujima, N.; Yamaguchi, T. *J. Phys. Soc. Jpn.* **1989**, *58*, 3290.
(48) Matos, M.; Maffeo, B.; Zerner, M. C. *J. Phys. B* **1982**, *15*, 7351.